Chemical Research in Toxicology

Article

pubs.acs.org/crt

Potential Metabolic Activation of a Representative C2-Alkylated Polycyclic Aromatic Hydrocarbon 6-Ethylchrysene Associated with the Deepwater Horizon Oil Spill in Human Hepatoma (HepG2) Cells

Meng Huang,[†] Clementina Mesaros,[‡] Suhong Zhang,[‡] Ian A. Blair,[†,‡] and Trevor M. Penning*[,†,‡]

[†]Center of Excellence in Environmental Toxicology and [‡]Center for Cancer Pharmacology, Department of Systems Pharmacology and Translational Therapeutics, Perelman School of Medicine, University of Pennsylvania, Philadelphia, Pennsylvania 19104-6160, United States

Supporting Information

ABSTRACT: Exposure to polycyclic aromatic hydrocarbons (PAHs) is the major human health hazard associated with the Deepwater Horizon oil spill. C2-Chrysenes are representative PAHs present in crude oil and could contaminate the food chain. We describe the metabolism of a C2-chrysene regioisomer, 6-ethylchrysene (6-EC), in human HepG2 cells. The structures of the metabolites were identified by HPLC-UV-fluorescence detection and LC-MS/MS. 6-EC-tetraol isomers were identified as signature metabolites of the diol-epoxide pathway. O-Monomethyl-O-monosulfonated-6-EC-catechol, its monohydroxy products, and *N*-acetyl-L-cysteine(NAC)-6-EC-ortho-quinone were discovered as signature metabolites of the ortho-quinone pathway. Potential dual metabolic activation of 6-EC involving the formation of bis-electrophiles, i.e., a mono-diol-epoxide and a mono-ortho-quinone within the same structure, bis-diol-epoxides, and bis-ortho-quinones was observed as well. The identification of 6-EC-tetraol, O-monomethyl-O-monosulfonated-6-EC-catechol, its monohydroxy products, and NAC-6-EC-ortho-quinone supports potential metabolic activation of 6-EC by P450 and AKR enzymes followed by metabolic detoxification of the ortho-quinone through interception of its redox cycling capability by catechol-O-methyltransferase and sulfotransferase enzymes. The tetraols and catechol conjugates could be used as biomarkers of human exposure to 6-EC resulting from oil spills.

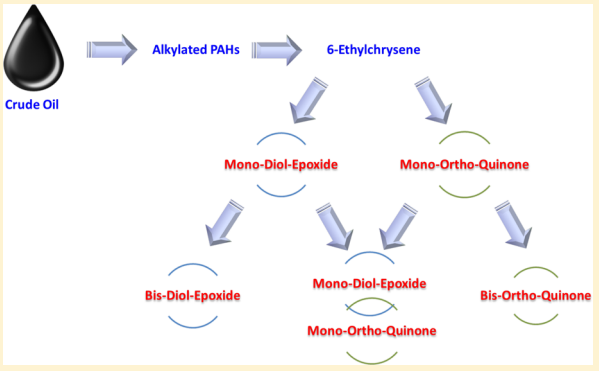

INTRODUCTION

The Deepwater Horizon oil spill in the Gulf of Mexico in 2010 was the largest release of crude oil in U.S. history.[1,2] Polycyclic aromatic hydrocarbons (PAHs), which are suspected human carcinogens, are among the most toxic and persistent components of crude oil.[3] According to their origins, PAHs are classified into pyrogenic PAHs arising from fossil fuel combustion and petrogenic PAHs that are unique to crude oil. Petrogenic PAHs differ in structure from that of pyrogenic PAHs (unsubstituted) in that they are either extensively alkylated or oxygenated to yield PAH-quinones.

Contamination of the food chain with petrogenic PAHs is a major hazard that would impact human health.[4] It is widely recognized that pyrogenic PAHs themselves are biologically inert and that their carcinogenic effects require metabolic activation to generate biologically reactive intermediates to form DNA adducts that result in mutations.[5] However, there is a paucity of information on the toxicological properties of petrogenic PAHs. In our previous studies, we described metabolic activation of a representative alkylated PAH 5-methylchrysene (regioisomer of C1-chrysenes) and a representative oxygenated PAH phenanthrene-9,10-quinone in human hepatoma (HepG2) cells.[6,7]

Alkylated PAH 6-ethylchrysene (6-EC) is a representative regioisomer of C2-chrysenes detected in the crude oil released from the Deepwater Horizon oil spill.[8,9] To our knowledge, there are no published accounts of the metabolic activation of 6-EC. In view of the fact that human liver is the major target organ for exposure to 6-EC following ingestion, we studied the metabolism of 6-EC in human HepG2 cells as a model to predict metabolism in primary human hepatocytes.

Four possible routes for the potential metabolic activation of 6-EC were considered to predict and identify its metabolites (Scheme 1). First, we predicted the diol-epoxide pathway, involving conversion of 6-EC to trans-dihydrodiols followed by formation of diol-epoxides, which can form DNA adducts or be hydrolyzed to the corresponding tetraols. Second, we predicted the ortho-quinone pathway, involving conversion of trans-dihydrodiols to catechols followed by either formation of conjugates, or their oxidation to ortho-quinones, which could be reduced back to the catechols to establish redox cycling that leads to oxidative DNA damage. The electrophilic ortho-quinone could also react with DNA or the most abundant

Received: January 28, 2016
Published: April 7, 2016

DOI: 10.1021/acs.chemrestox.6b00036
Chem. Res. Toxicol. 2016, 29, 991−1002

Scheme 1. Possible Metabolic Activation Pathways of 6-EC

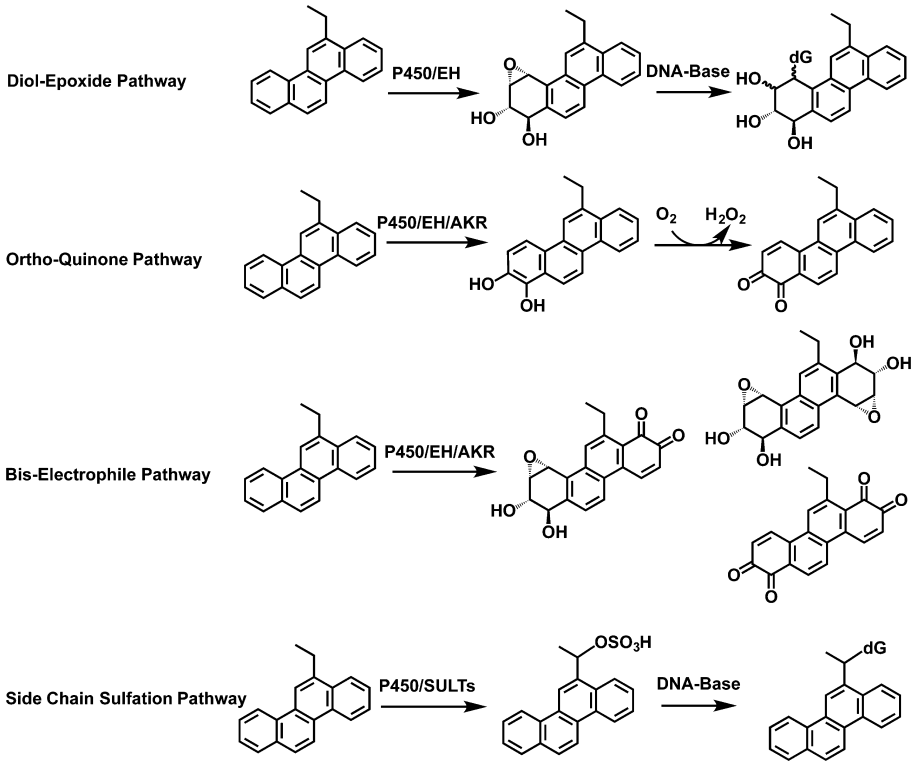

cellular nucleophile, glutathione (GSH), to form the GSH conjugates, which could be further metabolized into the cysteinylglycine (Cys-Gly) conjugates, cysteine (Cys) conjugates, and eventually *N*-acetyl-L-cysteine (NAC) conjugates. Third, as 6-EC contains two bay regions within its structure, a combination of these two potential metabolic activation pathways was also predicted. Fourth, we also predicted that hydroxylation on the side chain of the 6-ethyl group followed by formation of sulfate conjugates resulting in DNA adducts could be another potential metabolic activation pathway.

It was found that the metabolism of 6-EC involved the formation of mono-diol-epoxides, mono-ortho-quinones, and bis-electrophiles. Bis-electrophiles involved the formation of a mono-diol-epoxide and a mono-ortho-quinone on different terminal rings within the same structure, the formation of bis-diol-epoxides, and the formation of bis-ortho-quinones. We conclude that the diol-epoxide pathway, the ortho-quinone pathway, and their combination likely lead to the potential metabolic activation of 6-EC following ingestion. 6-EC-tetraols and 6-EC-catechol conjugates represent human exposure biomarkers for 6-EC that may result from consuming seafood contaminated by crude oil spills.

MATERIALS AND METHODS

Caution! *All PAHs are potentially hazardous and should be handled in accordance with the National Institutes of Health Guidelines for the Laboratory Use of Chemical Carcinogens.*

Chemicals and Reagents. Cell culture media and reagents were all obtained from Invitrogen Co. (Carlsbad, CA) except for fetal bovine serum, which was purchased from Hyclone (Logan, UT). 6-EC was purchased from AccuStandard Inc. (New Haven, CT). All other chemicals used were of the highest grade available, and all solvents were HPLC grade.

Cell Culture. HepG2 (human hepatocellular carcinoma) cells were obtained from American Type Culture Collection and maintained as previously described.[6] Cultured cells with a passage number of 10−20 were used in the experiments to reduce variability due to long-term culture conditions. Cultured cells were authenticated by short-terminal repeat DNA analysis and were mycoplasma-free (DNA Diagnostics Center Medical, Fairfield, OH).

Detection and Identification of 6-EC Metabolites in HepG2 Cells. Confluent HepG2 cells were plated in a 6-well plate (~5×10^6). The cells were washed twice and then treated with MEM (without phenol red) containing 10 mM glucose and 1 μM 6-EC (DMSO, 0.2% v/v). The culture media were collected at 0 and 24 h and subsequently acidified with 0.1% formic acid before extraction as previously described.[6] The extract from the cell culture media was reconstituted in 150 μL of methanol.

For HPLC-UV-FLR analysis, a 10 μL aliquot of the reconstituted extract was analyzed on a tandem Waters Alliance 2695 chromatographic system with a Waters 2996 photodiode array (PDA) detector and a Waters 2475 multi λ fluorescence (FLR) detector (Waters Corporation, Milford, MA). Separations were accomplished on a Zorbax-ODS C18 analytical column (5 μm, 4.6 mm × 250 mm) with a Zorbax-ODS analytical guard column (5 μm, 4.6 mm × 12.5 mm) (DuPont Co., Wilmington, DE) at ambient temperature. The mobile phase consisted of 5 mM ammonium acetate and 0.1% trifluoroacetic acid (TFA) (v/v) in H_2O (solvent A) and 5 mM ammonium acetate and 0.1% TFA in acetonitrile (solvent B) and was delivered at a flow rate of 0.5 mL/min. The linear gradient elution program was as follows: 5 to 95% B over 30 min, followed by an isocratic hold at 95% B for another 10 min. At 40 min, B was returned to 5% in 1 min, and the column was equilibrated for 19 min before the next injection. The total run time for each analysis was 60 min. Eluants from the column were introduced sequentially into the PDA and FLR detectors. Excitation (λ_{ex}) and emission (λ_{em}) wavelengths for the FLR detector were set at 269 and 366 nm, respectively, based on the spectral properties of 6-EC (Figure S1). The optimal pair of λ_{ex} and λ_{em} of 6-EC was employed to detect its metabolites based on the assumption that most 6-EC metabolites show fluorescence signals at these wavelengths.

For ion trap LC-MS/MS analysis, a 10 μL aliquot of the reconstituted extract was analyzed on a Waters Alliance 2690 HPLC

DOI: 10.1021/acs.chemrestox.6b00036
Chem. Res. Toxicol. 2016, 29, 991−1002

system (Waters Corporation, Milford, MA) coupled to a Finnigan LTQ linear ion trap mass spectrometer (Thermo Scientific, San Jose, CA). The column, mobile phase, flow rate, and linear gradient elution program were the same as those described above. During LC-MS/MS analysis, up to 10 min of the initial flow was diverted to waste before evaluation of eluants. The mass spectrometer was operated in both positive and negative ion modes with an electrospray ionization (ESI) source. Eluants were monitored on the LTQ using product ion scan (MS^2), subsequent MS/MS/MS (MS^3), and pseudo selected reaction monitoring (SRM) modes. The mass spectrometry parameters included spray voltage (3 kV in positive ion mode and 5 kV in negative ion mode), sheath gas flow rate (40 arbitrary units in both ion modes), auxiliary gas flow rate (15 arbitrary units in both ion modes), capillary temperature (275 °C in both ion modes), capillary voltage (38 V in positive ion mode and −19 V in negative ion mode), and tube lens (20 V in positive ion mode and −22.05 V in negative ion mode). An isolation width of 3 bracketed around the m/z of interest, activation Q of 0.25, and activation time of 30 ms were used for data acquisition. Xcalibur software, version 2.0 (Thermo Scientific, San Jose, CA), was used to control the LC-MS/MS system and to process data. The preliminary information on metabolite structures was obtained by interpreting the corresponding MS^2 and MS^3 spectra of 6-EC metabolites from ion trap LC-MS/MS.

In some instances, another 5 μL aliquot of the reconstituted extract was analyzed on a nano-Acquity ultra-performance liquid chromatography (UPLC) system (Waters Corporation, Milford, MA) coupled to a LTQ Orbitrap XL mass spectrometer (Thermo Scientific, San Jose, CA). Separations were accomplished on a nano-UPLC C18 column (1.7 μm BEH130, 150 μm × 100 mm) (Waters Corporation, Milford, MA) at 50 °C. The mobile phase consisted of 0.1% formic acid (v/v) in H_2O (solvent A) and 0.1% formic acid (v/v) in acetonitrile (solvent B) and was delivered at a flow rate of 1.6 μL/min. The linear gradient elution program was as follows: an isocratic hold at 5% B for 5 min, 5 to 95% B over 30 min, followed by an isocratic hold at 95% B for another 10 min. At 46 min, B was returned to 5% in 2 min, and the column was equilibrated for 12 min before the next injection. The total run time for each analysis was 60 min. The mass spectrometer was operated in positive and negative ion modes with a nano-electrospray ionization (nano-ESI) source after accurate calibration with the manufacturer's calibration mixture. The ionization voltage was set to 1.5 kV, and the capillary temperature was set to 200 °C. Full scan spectra were acquired with a resolving power of 60 000 full width at half-maximum in the mass range from m/z 100 to 600. Lists of accurate masses of the potential 6-EC metabolites were used to detect the formation of bis-electrophiles containing both a diol-epoxide and an ortho-quinone within the same structure in Table 1, the formation of bis-diol-epoxides in Table 2, and the formation of bis-ortho-quinones in Table 3. Xcalibur software, version 2.0 (Thermo Scientific, San Jose, CA), was used to control the Orbitrap mass spectrometer and to process data.

RESULTS

Detection of 6-EC Metabolites in HepG2 Cells by HPLC-UV-FLR. Comparison of UV chromatograms at λ_{max} 269 nm at 0 h (Figure 1A) and 24 h (Figure 1B) showed that nine metabolites of 6-EC were detected in the organic phase of the ethyl acetate-extracted acidified media from HepG2 cells. The peak attributed to 6-EC at 0 h was almost completely absent at 24 h, suggesting that 6-EC was rapidly metabolized by HepG2 cells over this time course. The corresponding UV spectra of the nine metabolites were extracted from the PDA detector and are shown in Figure S2. The UV spectra of metabolites 4−8 were similar to that of 6-EC, showing that aromaticity has been retained, whereas metabolites 2 and 3 were predicted to have lost their aromaticity.

Comparison of FLR chromatograms at λ_{ex} 269 nm and λ_{em} 366 nm at 0 h (Figure 1C) and 24 h (Figure 1D) showed that there were seven fluorescence peaks in Figure 1D, corresponding to metabolites 2−8 in Figure 1B, thus validating the presence of a fluorophore. The peaks corresponding to metabolites 1 and 9 were detected only in the UV chromatogram (Figure 1B) but not in the FLR chromatogram (Figure 1D), suggesting a loss of the 6-EC ring fluorophore.

Table 1. Accurate Masses of Potential 6-EC Metabolites in HepG2 Cells That Result from the Formation of Bis-Electrophiles Containing Both a Diol-Epoxide and an Ortho-Quinone

6-EC metabolites	molecular formula	positive mode	negative mode
tetraol + O-quinone	$C_{20}H_{18}O_6$	355.1182	353.1025
monodehydrated tetraol + O-quinone	$C_{20}H_{16}O_5$	337.1076	335.0919
bis-dehydrated tetraol + O-quinone	$C_{20}H_{14}O_4$	319.0970	317.0814
tetraol + O-methyl catechol	$C_{21}H_{22}O_6$	371.1495	369.1338
monodehydrated tetraol + O-methyl catechol	$C_{21}H_{20}O_5$	353.1389	351.1232
bis-dehydrated tetraol + O-methyl catechol	$C_{21}H_{18}O_4$	335.1283	333.1127
tetraol + O-sulfonated catechol	$C_{20}H_{20}O_9S$	437.0906	435.0750
monodehydrated tetraol + O-sulfonated catechol	$C_{20}H_{18}O_8S$	419.0801	417.0644
bis-dehydrated tetraol + O-sulfonated catechol	$C_{20}H_{16}O_7S$	401.0695	399.0538
tetraol + O-glucuronosyl catechol	$C_{26}H_{28}O_{12}$	533.1659	531.1503
monodehydrated tetraol + O-glucuronosyl catechol	$C_{26}H_{26}O_{11}$	515.1553	513.1397
bis-dehydrated tetraol + O-glucuronosyl catechol	$C_{26}H_{24}O_{10}$	497.1448	495.1291
tetraol + O-methyl-O-sulfonated catechol	$C_{21}H_{22}O_9S$	451.1063	449.0906
monodehydrated tetraol + O-methyl-O-sulfonated catechol	$C_{21}H_{20}O_8S$	433.0957	431.0801
bis-dehydrated tetraol + O-methyl-O-sulfonated catechol	$C_{21}H_{18}O_7S$	415.0851	413.0695

Evidence for the Diol-Epoxide Pathway. Identification of O-monosulfonated-6-EC-dihydrodiol, 6-EC-dihydrodiol, and 6-EC-tetraol indicated the occurrence of the diol-epoxide pathway as a potential metabolic route of activation of 6-EC in HepG2 cells.

A single isomer of monodehydrated O-monosulfonated-6-EC-dihydrodiol with the retention time of 23.42 min was detected by comparing the pseudo SRM chromatograms (m/z 351 → 271) at 0 h (Figure 2A) and 24 h (Figure 2B) in the negative ion mode. The corresponding MS^2 spectrum (m/z 351) of this metabolite showed the characteristic loss of the sulfate group (80 amu) from the deprotonated molecular ion (Figure 2C), and the MS^3 spectrum (m/z 351 → 271 →) of this metabolite showed the subsequent loss of one CH_3 group from the alkyl side chain (Figure 2D). The specific position of the O-monosulfonated-dihydrodiol could not be assigned using mass spectrometry.

Three isomers of 6-EC-dihydrodiols and three isomers of monodehydrated 6-EC-dihydrodiols were detected in HepG2 cells with identical retention times by monitoring the extracted ion chromatograms of the Orbitrap full scan at 0 and 24 h in the positive ion mode (Figure S3). MS spectra of these isomers provided the accurate masses and molecular formulas of 6-EC-dihydrodiols and their monodehydrated products with acceptable ppm values (Figure S3). The presence of these isomers suggests saturation of 6-EC on both terminal benzo rings.

Two isomers of bis-dehydrated 6-EC-tetraols at 17.72 and 19.04 min were detected by monitoring the MS^2 chromato-

DOI: 10.1021/acs.chemrestox.6b00036
Chem. Res. Toxicol. 2016, 29, 991−1002

Table 2. Accurate Masses of Potential 6-EC Metabolites in HepG2 Cells That Result from the Formation of Bis-Diol-Epoxides

6-EC metabolites	molecular formula	positive mode	negative mode
tetraol + tetraol	$C_{20}H_{24}O_8$	393.1549	391.1393
monodehydrated tetraol + tetraol	$C_{20}H_{22}O_7$	375.1444	373.1287
monodehydrated tetraol + monodehydrated tetraol (or bis-dehydrated tetraol + tetraol)	$C_{20}H_{20}O_6$	357.1338	355.1182
monodehydrated tetraol + bis-dehydrated tetraol	$C_{20}H_{18}O_5$	339.1232	337.1076
bis-dehydrated tetraol + bis-dehydrated tetraol	$C_{20}H_{16}O_4$	321.1127	319.0970
tetraol + O-sulfonated tetraol	$C_{20}H_{24}O_{11}S$	473.1118	471.0961
monodehydrated tetraol + O-sulfonated tetraol	$C_{20}H_{22}O_{10}S$	455.1012	453.0855
monodehydrated tetraol + monodehydrated O-sulfonated tetraol (or bis-dehydrated tetraol + O-sulfonated tetraol)	$C_{20}H_{20}O_9S$	437.0906	435.0750
monodehydrated tetraol + bis-dehydrated O-sulfonated tetraol	$C_{20}H_{18}O_8S$	419.0801	417.0644
bis-dehydrated tetraol + bis-dehydrated O-sulfonated tetraol	$C_{20}H_{16}O_7S$	401.0695	399.0538
tetraol + O-glucuronosyl tetraol	$C_{26}H_{32}O_{14}$	569.1870	567.1714
monodehydrated tetraol + O-glucuronosyl tetraol	$C_{26}H_{30}O_{13}$	551.1765	549.1608
monodehydrated tetraol + monodehydrated O-glucuronosyl tetraol (or bis-dehydrated tetraol + O-glucuronosyl tetraol)	$C_{26}H_{28}O_{12}$	533.1659	531.1503
monodehydrated tetraol + bis-dehydrated O-glucuronosyl tetraol	$C_{26}H_{26}O_{11}$	515.1553	513.1397
bis-dehydrated tetraol + bis-dehydrated O-glucuronosyl tetraol	$C_{26}H_{24}O_{10}$	497.1448	495.1291

Table 3. Accurate Masses of Potential 6-EC Metabolites in HepG2 Cells That Result from the Formation of Bis-Ortho-Quinones

6-EC metabolites	molecular formula	positive mode	negative mode
O-quinone + O-quinone	$C_{20}H_{12}O_4$	317.0814	315.0657
O-quinone + O-methyl catechol	$C_{21}H_{16}O_4$	333.1127	331.0970
O-quinone + O-sulfonated catechol	$C_{20}H_{14}O_7S$	399.0538	397.0382
O-quinone + O-glucuronosyl catechol	$C_{26}H_{22}O_{10}$	495.1291	493.1135
O-quinone + O-methyl-O-sulfonated catechol	$C_{21}H_{16}O_7S$	413.0695	411.0538
O-methyl catechol + O-methyl catechol	$C_{22}H_{20}O_4$	349.1440	347.1283
O-methyl catechol + O-sulfonated catechol	$C_{21}H_{18}O_7S$	415.0851	413.0695
O-methyl catechol + O-glucuronosyl catechol	$C_{27}H_{26}O_{10}$	511.1604	509.1448
O-sulfonated catechol + O-sulfonated catechol	$C_{20}H_{16}O_{10}S_2$	481.0263	479.0107
O-sulfonated catechol + O-glucuronosyl catechol	$C_{26}H_{24}O_{13}S$	577.1016	575.0859
O-glucuronosyl catechol + O-glucuronosyl catechol	$C_{32}H_{32}O_{16}$	673.1769	671.1612

grams (m/z 289) at 0 and 24 h in the positive ion mode (Table 4). The corresponding MS^2 spectra (m/z 289) of these metabolites showed the sequential loss of H_2O (18 amu), CO (28 amu), and CH_3 (15 amu) from the protonated molecular ion (Table 4). Comparison of the retention times of bis-dehydrated 6-EC-tetraols with metabolites 2 and 3 by HPLC-UV-FLR in Figure 1 showed good agreement.

A single isomer of a monodehydrated 6-EC-tetraol and a single isomer of a bis-dehydrated 6-EC-tetraol were detected in HepG2 cells with different retention times by monitoring the extracted ion chromatograms of the Orbitrap full scan at 0 and 24 h in the positive ion mode (Figure S4). Because 6-EC is asymmetric, there are two possible regioisomeric 6-EC-tetraols: those that come from 6-EC-*trans*-1,2-dihydrodiol and those that come from 6-EC-*trans*-7,8-dihydrodiol. The resulting tetraols and their absolute configurations cannot be assigned using mass spectrometry.

Evidence for the Ortho-Quinone Pathway. Identification of 6-EC-dihydrodiol, O-monosulfonated-6-EC-catechol, O-monomethyl-O-monosulfonated-6-EC-catechol, monohydroxy-O-monomethyl-O-monosulfonated-6-EC-catechol, 6-EC-dione, monohydroxy-6-EC-dione, and NAC-6-EC-ortho-quinone indicated the occurrence of the ortho-quinone pathway as a potential route of metabolic activation of 6-EC in HepG2 cells.

A single isomer at 24.38 min corresponding to either an O-monosulfonated-6-EC-catechol or an O-monosulfonated-6-EC-bis-phenol was detected by monitoring the pseudo SRM chromatograms (m/z 367 → 287) at 0 h (Figure 3A) and 24 h (Figure 3B) in the negative ion mode. The corresponding MS^2 spectrum (m/z 367) of this metabolite showed the characteristic loss of the sulfate group (80 amu) from the deprotonated molecular ion (Figure 3C), and the MS^3 spectrum (m/z 367 → 287 →) of this metabolite showed the subsequent loss of one CH_3 group (Figure 3D). Comparison of the retention time of this peak with that of metabolite 7 by HPLC-UV-FLR in Figure 1 showed that they were in agreement. Mass spectrometry cannot distinguish a catechol from a bis-phenol. However, we favor formation of the O-monosulfonated-6-EC-catechol isomer because it would be derived from the reduction of either 6-EC-1,2-dione or 7,8-dione. Both the intermediate 6-EC-dihydrodiol and 6-EC-dione were detected in this study.

Two isomers of O-monomethyl-O-monosulfonated-6-EC-catechols at 21.12 and 24.05 min were detected by monitoring the pseudo SRM chromatograms (m/z 381 → 301) at 0 h (Figure 4A) and 24 h (Figure 4B) in the negative ion mode, which showed the loss of the sulfate group (80 amu) from the deprotonated molecular ion. The MS^3 spectrum (m/z 381 → 301 →) of the isomer peak at 24.05 min showed the characteristic losses of CH_3 and CH_2CH_3 groups (Figure 4C), suggesting that the CH_3 group was not cleaved from the CH_2CH_3 side chain of 6-EC and was due to the occurrence of O-methylation. The unique biotransformation of O-methylation strongly indicated the formation of the catechol, thus confirming the potential metabolic activation of 6-EC via the ortho-quinone pathway. Although the specific position of catechol conjugation, the methyl group, and the sulfate group on 6-EC-catechols could not be assigned using mass spectrometry, it is likely that only 6-EC-1,2-catechols or 7,8-catechols were formed. Comparison of the retention time of the major isomer peak at 24.05 min with that of metabolite 6 by HPLC-UV-FLR in Figure 1 showed good concordance.

DOI: 10.1021/acs.chemrestox.6b00036
Chem. Res. Toxicol. 2016, 29, 991−1002

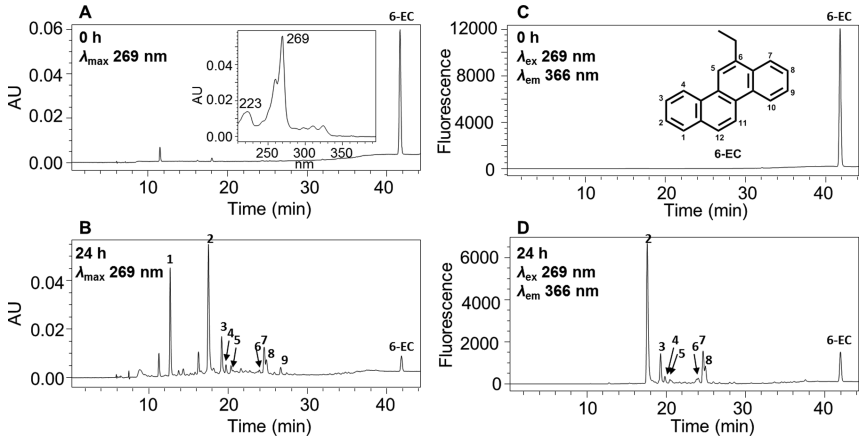

Figure 1. HPLC detection of 6-EC metabolites in human HepG2 cells. (A) UV chromatogram at λ_{max} 269 nm at 0 h. (B) UV chromatogram at λ_{max} 269 nm at 24 h. (C) FLR chromatogram at λ_{ex} 269 nm and λ_{em} 366 nm at 0 h. (D) FLR chromatogram at λ_{ex} 269 nm and λ_{em} 366 nm at 24 h. Human HepG2 cells ($\sim 5 \times 10^6$) were treated with 6-EC (1 μM, 0.2% (v/v) DMSO) in MEM (without phenol red) containing 10 mM glucose. The cell media were collected at 0 and 24 h and subsequently acidified with 0.1% formic acid before extraction with ethyl acetate. The extracts were analyzed by HPLC-UV-FLR.

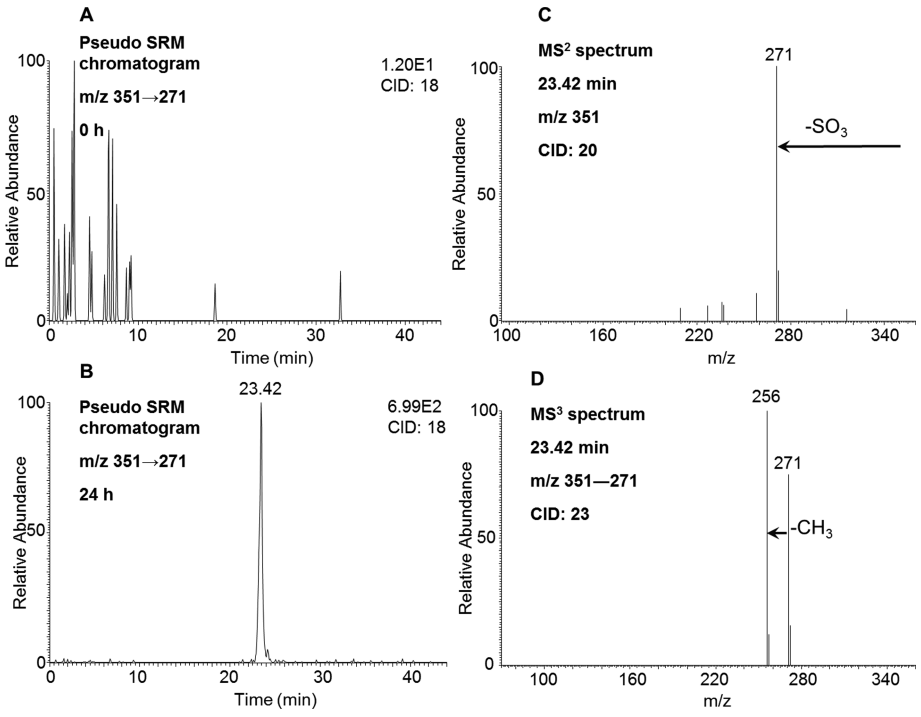

Figure 2. Detection of monodehydrated O-monosulfonated-6-EC-dihydrodiol in human HepG2 cells. (A) Extracted ion chromatogram of pseudo SRM transition at 0 h. (B) Extracted ion chromatogram of pseudo SRM transition at 24 h. (C) MS^2 spectrum of the peak at 23.42 min. (D) MS^3 spectrum of the peak at 23.42 min. The samples were prepared as described in the caption to Figure 1 and were subsequently analyzed on an ion trap LC-MS/MS.

Five isomers of monohydroxy-O-monomethyl-O-monosulfonated-6-EC-catechols at 19.51, 19.93, 20.47, 24.05, and 25.18 min were detected by monitoring the pseudo SRM chromatograms (m/z 397 → 317) at 0 h (Figure 5A) and 24 h (Figure 5B) in the negative ion mode, which showed the loss of the sulfate group (80 amu) from the deprotonated molecular ion. The MS^3 spectrum (m/z 397 → 317 →) of the isomer peak at 19.93 min showed the characteristic losses of CH_3 and CH_2CH_3 (Figure 5C), suggesting that the CH_3 group was not cleaved from the CH_2CH_3 side chain of 6-EC and was due to the occurrence of O-methylation. The unique biotransformation of O-methylation strongly indicated the formation of the catechol, thus confirming the potential metabolic activation of 6-EC by the ortho-quinone pathway. As the loss of CH_2CH_2OH was not observed, this ruled out activation of 6-EC by a combination of the ortho-quinone pathway and side chain hydroxylation. Although the specific position of catechol conjugation, the hydroxyl group, the methyl group, and the sulfate group on 6-EC-catechols could not be assigned using mass spectrometry, it is likely that only 6-EC-1,2-catechols or 7,8-catechols were formed. Comparison of the retention times of the isomer peaks at 19.93, 20.47, 25.18 min with those of metabolites 4, 5, and 8 by HPLC-UV-FLR in Figure 1 showed that they were in agreement.

DOI: 10.1021/acs.chemrestox.6b00036
Chem. Res. Toxicol. 2016, 29, 991−1002

Table 4. Mass Transitions for 6-Ethylchrysene Metabolites in HepG2 Cells

metabolite no.	6-EC metabolites	retention time (min)	mode	*m/z*
–	dehydrated O-sulfonated dihydrodiol	23.42	negative	351 $[M - H]^-$, 271 $[M - H - SO_3]^-$, 256 $[M - H - SO_3 - CH_3]^-$
2, 3	bis-dehydrated tetraol	17.72, 19.04	positive	289 $[M + H]^+$, 271 $[M + H - H_2O]^+$, 243 $[M + H - H_2O - CO]^+$, 228 $[M + H - H_2O - CO - CH_3]^+$, 215 $[M + 2H - H_2O - CO - CH_2CH_3]^+$
7	O-sulfonated catechol [O-sulfonated bis-phenol]	24.38	negative	367 $[M - H]^-$, 287 $[M - H - SO_3]^-$, 272 $[M - H - SO_3 - CH_3]^-$
6	O-methyl-O-sulfonated catechol	21.12, 24.05	negative	381 $[M - H]^-$, 301 $[M - H - SO_3]^-$, 286 $[M - H - SO_3 - CH_3]^-$, 257 $[M - H - SO_3 - CH_3 - CH_2CH_3]^-$
4, 5, 8	monohydroxy-O-methyl-O-sulfonated catechol	19.93, 20.47, 25.18	negative	397 $[M - H]^-$, 317 $[M - H - SO_3]^-$, 302 $[M - H - SO_3 - CH_3]^-$, 273 $[M - H - SO_3 - CH_3 - CH_2CH_3]^-$
–	quinone	34.06	positive	287 $[M + H]^+$, 269 $[M + H - H_2O]^+$, 259 $[M + H - CO]^+$, 244 $[M + H - CO - CH_3]^+$, 231 $[M + H - 2CO]^+$
–	monohydroxy-quinone	29.58	positive	302 $[M + H - \bullet H]^+$, 274 $[M + H - CO - \bullet H]^+$, 246 $[M + H - 2CO - \bullet H]^+$, 218 $[M + H - 3CO - \bullet H]^+$
–	NAC-ortho-quinone	32.99	negative	446 $[M - H]^-$, 418 $[M - H - CO]^-$, 317 $[M - H - CH_2{=}C(NHCOCH_3)COOH]^-$, 288 $[M - H - CH_2{=}C(NHCOCH_3)COOH{-}CH_2CH_3]^-$

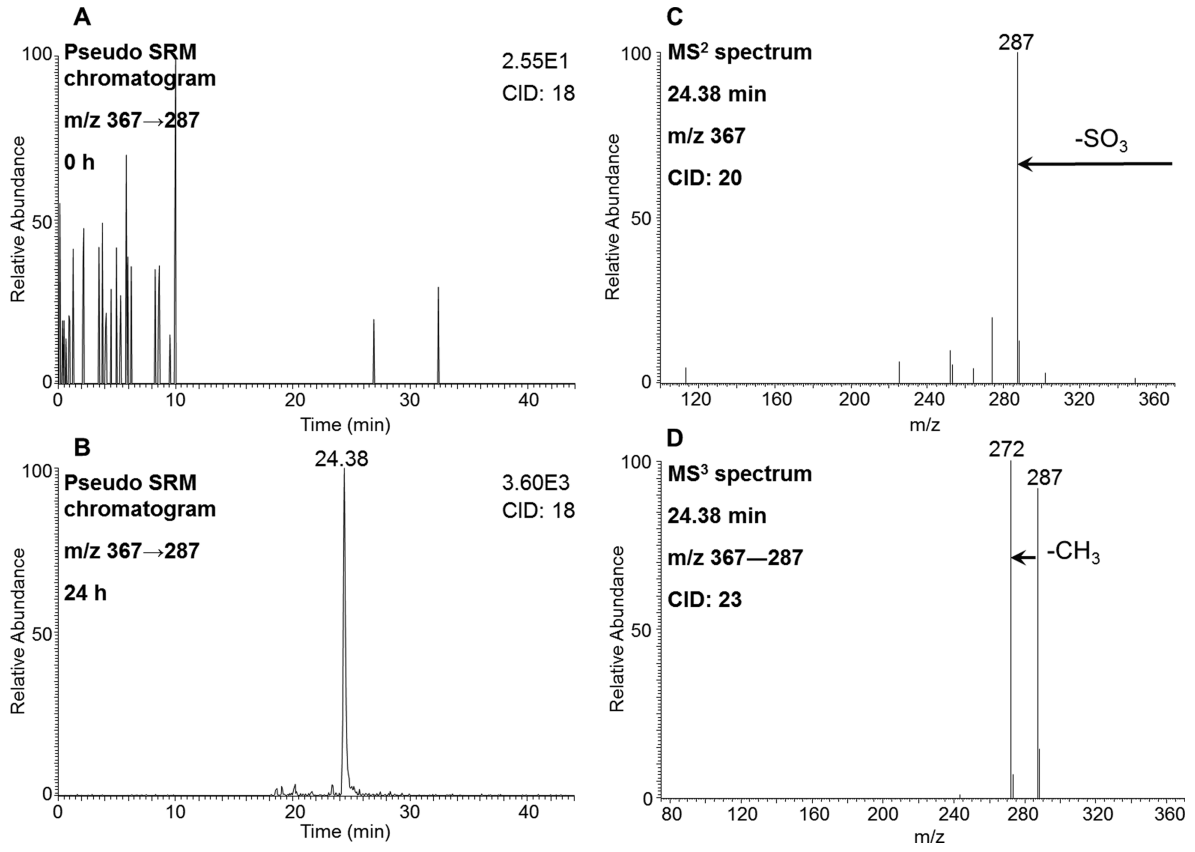

Figure 3. Detection of either an O-monosulfonated-6-EC-catechol or an O-monosulfonated-6-EC-bis-phenol in human HepG2 cells. (A) Extracted ion chromatogram of pseudo SRM transition at 0 h. (B) Extracted ion chromatogram of pseudo SRM transition at 24 h. (C) MS^2 spectrum of the peak at 24.38 min. (D) MS^3 spectrum of the peak at 24.38 min. The samples were prepared as described in the caption to Figure 1 and were subsequently analyzed on an ion trap LC-MS/MS.

Two peaks at 24.41 and 34.06 min corresponding to 6-EC-dione were detected by comparing the pseudo SRM chromatograms (*m/z* 287 → 259) at 0 h (Figure 6A) and 24 h (Figure 6B) in the positive ion mode. The respective MS^2 spectra (*m/z* 287) of these two metabolites showed the characteristic loss of CO (28 amu) from the protonated molecular ion, and a representative MS^2 spectrum of the metabolite with a retention time of 34.06 min is shown in Figure 6C. The MS^3 spectrum (*m/z* 287 → 259 →) of this metabolite showed the characteristic loss of a second CO and the loss of CH_3 (Figure 6D). The sequential loss of two CO groups supported the presence of either an ortho-quinone or a remote quinone, which cannot be distinguished on the basis of mass spectrometry.

A single isomer of monohydroxy-6-EC-dione at 29.58 min was detected by comparing the pseudo SRM chromatograms (*m/z* 303 → 274) at 0 h (Figure 7A) and 24 h (Figure 7B) in the positive ion mode. The corresponding MS^2 spectrum (*m/z* 303) of this metabolite (Figure 7C) showed the characteristic loss of CO (28 amu) plus one hydrogen from the protonated molecular ion. The MS^3 spectrum (*m/z* 303 → 274 →) of this metabolite (Figure 7D) showed another characteristic loss of

DOI: 10.1021/acs.chemrestox.6b00036
Chem. Res. Toxicol. 2016, 29, 991−1002

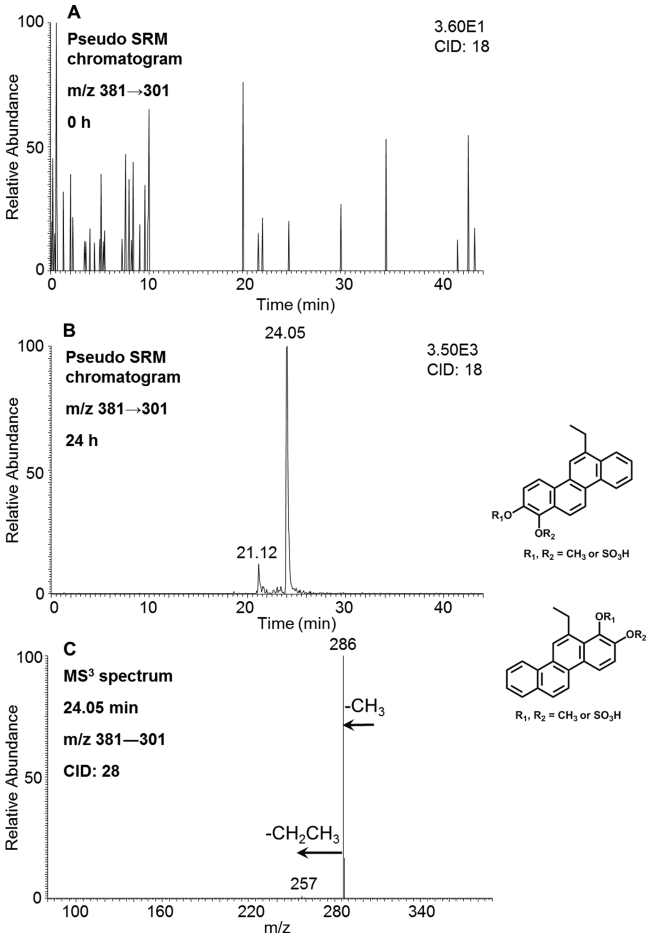

Figure 4. Detection of O-monomethyl-O-monosulfonated-6-EC-catechols in human HepG2 cells. (A) Extracted ion chromatogram of pseudo SRM transition at 0 h. (B) Extracted ion chromatogram of pseudo SRM transition at 24 h. (C) MS^3 spectrum of the peak at 24.05 min. The samples were prepared as described in the caption to Figure 1 and were subsequently analyzed on an ion trap LC-MS/MS.

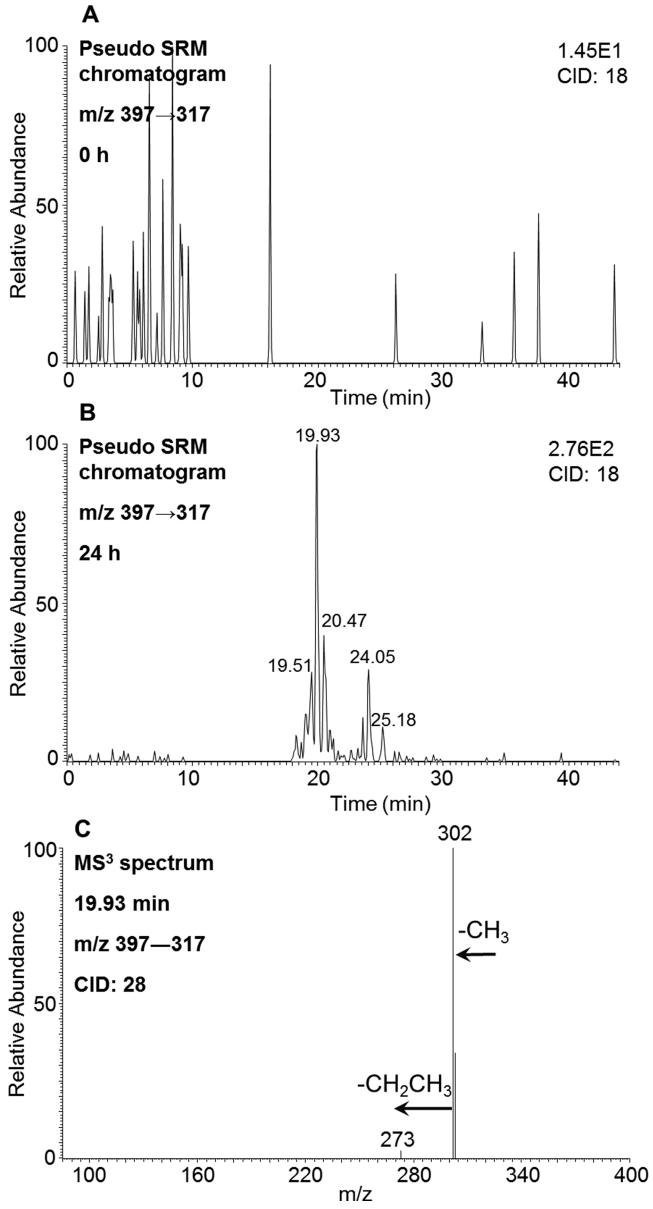

Figure 5. Detection of monohydroxy-O-monomethyl-O-monosulfonated-6-EC-catechol isomers in human HepG2 cells. (A) Extracted ion chromatogram of pseudo SRM transition at 0 h. (B) Extracted ion chromatogram of pseudo SRM transition at 24 h. (C) MS^3 spectrum of the peak at 19.93 min. Similar MS^3 spectra were obtained for the remaining isomers. The samples were prepared as described in the caption to Figure 1 and were subsequently analyzed on an ion trap LC-MS/MS.

CO. Monohydroxy-6-EC-dione could be derived from either an ortho-quinone or a remote quinone, and these alternatives cannot be distinguished on the basis of mass spectrometry. As the loss of CH_2CH_2OH was not observed, this ruled out activation of 6-EC by a combination of the ortho-quinone pathway and side chain hydroxylation.

A single isomer of NAC-6-EC-ortho-quinone at 32.99 min was detected by monitoring the MS^2 chromatograms (m/z 446) at 0 and 24 h in the negative ion mode (Table 4). The corresponding MS^2 spectrum (m/z 446) of this metabolite showed the characteristic loss of CO (28 amu) from the deprotonated molecular ion and the characteristic loss of 129 amu resulting from a cleavage of the thioether bond,[10] followed by the loss of CH_2CH_3 side chain (Table 4). The unique biotransformation of NAC conjugation strongly indicated the formation of the ortho-quinone, thus confirming a potential route of metabolic activation of 6-EC via the ortho-quinone pathway. The specific position of NAC conjugation on 6-EC-ortho-quinone could not be assigned using mass spectrometry.

Evidence for the Bis-Electrophile Pathway. Evidence for potential dual metabolic activation of 6-EC in HepG2 cells to form a bis-electrophile containing a diol-epoxide and an ortho-quinone within the same structure was obtained. Two isomers of tetrahydroxy-O-monomethyl-6-EC-catechol were detected by comparing the extracted ion chromatograms of the Orbitrap full scan at 0 and 24 h in the negative ion mode (Figure 8). In particular, the unique biotransformation of O-methylation strongly indicated the formation of the catechol, thus confirming the occurrence of ortho-quinone pathway. The specific positions of the hydroxy groups of the tetraol and O-monomethyl-catechol could not be assigned using mass spectrometry.

A bis-tetraol was detected by identification of two bis-dehydrated-tetraols in HepG2 cells by comparing the extracted ion chromatograms of Orbitrap full scan at 0 and 24 h in the positive ion mode (Figure S5), indicating the occurrence of

DOI: 10.1021/acs.chemrestox.6b00036
Chem. Res. Toxicol. 2016, 29, 991−1002

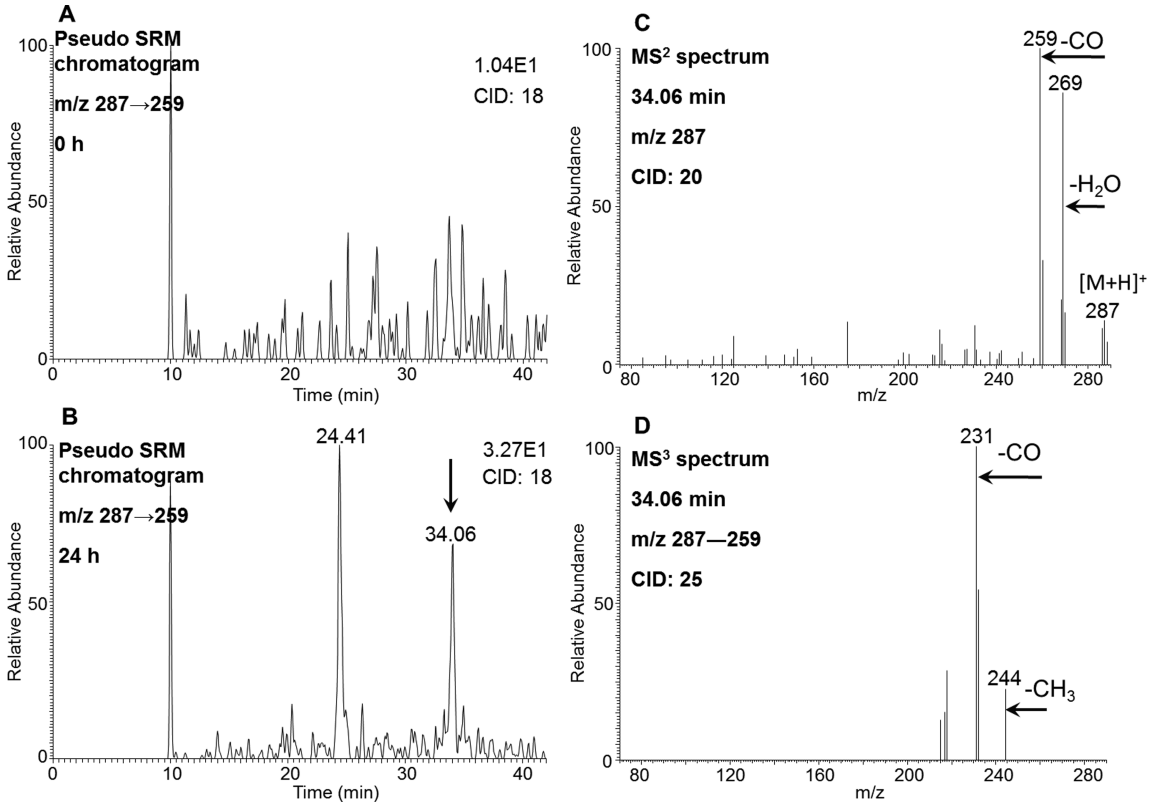

Figure 6. Detection of 6-EC-dione in human HepG2 cells. (A) Extracted ion chromatogram of pseudo SRM transition at 0 h. (B) Extracted ion chromatogram of pseudo SRM transition at 24 h. (C) MS^2 spectrum of the peak at 34.06 min. (D) MS^3 spectrum of the peak at 34.06 min. The samples were prepared as described in the caption to Figure 1 and were subsequently analyzed on an ion trap LC-MS/MS. Another peak with a retention time of 24.41 min with a relatively high polarity could be an isomer of O-monosulfonated-6-EC-catechol, which could undergo cleavage of its sulfate conjugate in the mass spectrometer, followed by auto-oxidation, and thus result in the detection of quinone instead.

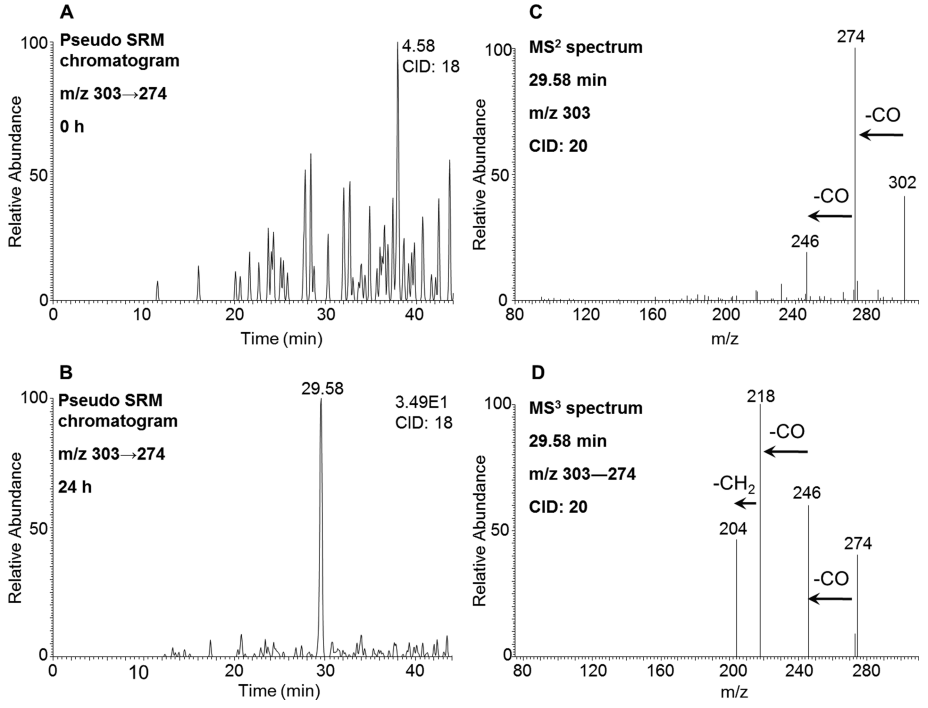

Figure 7. Detection of monohydroxy-6-EC-dione in human HepG2 cells. (A) Extracted ion chromatogram of pseudo SRM transition at 0 h. (B) Extracted ion chromatogram of pseudo SRM transition at 24 h. (C) MS^2 spectrum of the peak at 29.58 min. (D) MS^3 spectrum of the peak at 29.58 min. The samples were prepared as described in the caption to Figure 1 and were subsequently analyzed on an ion trap LC-MS/MS.

DOI: 10.1021/acs.chemrestox.6b00036
Chem. Res. Toxicol. 2016, 29, 991−1002

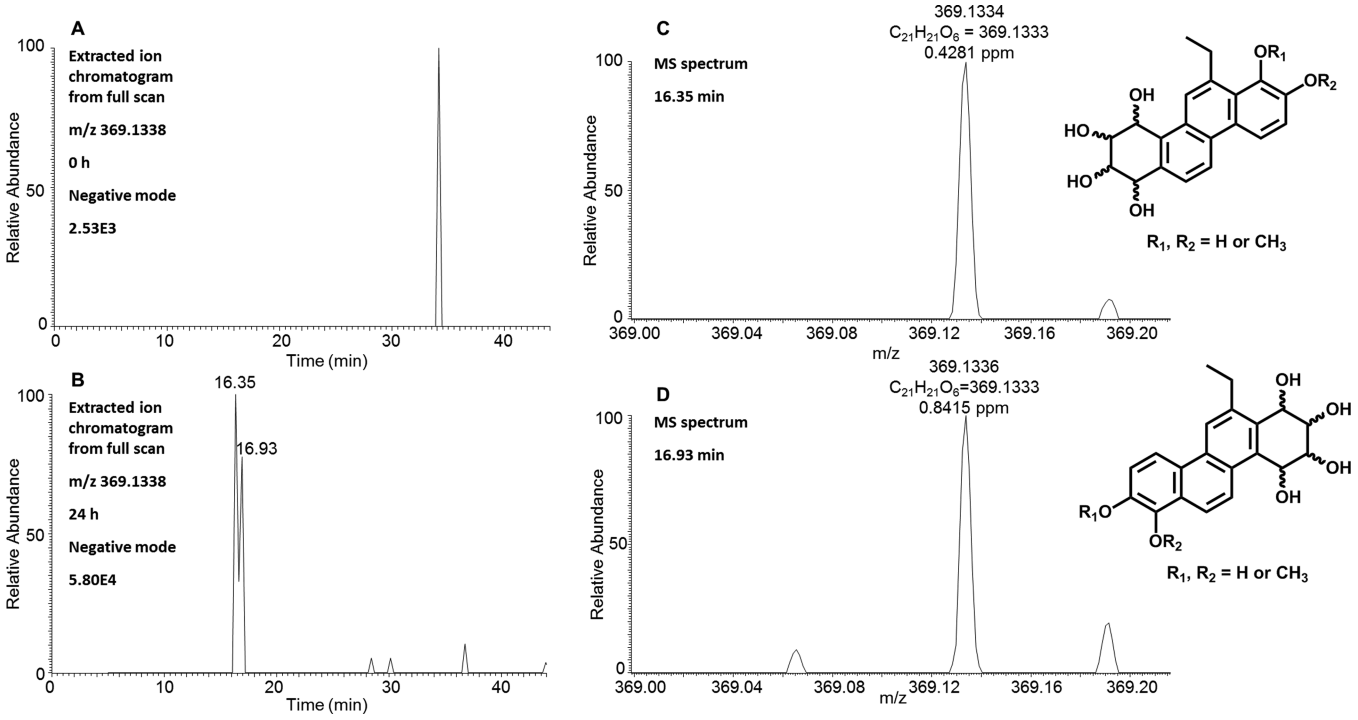

Figure 8. Detection of tetrahydroxy-O-monomethyl-6-EC-catechols in human HepG2 cells. (A) Extracted ion chromatogram of Orbitrap full scan at 0 h. (B) Extracted ion chromatogram of Orbitrap full scan at 24 h. (C) MS spectrum of the peak at 16.35 min. (D) MS spectrum of the peak at 16.93 min.

Scheme 2. Proposed Metabolic Pathway of 6-EC in Human HepG2 Cells[a]

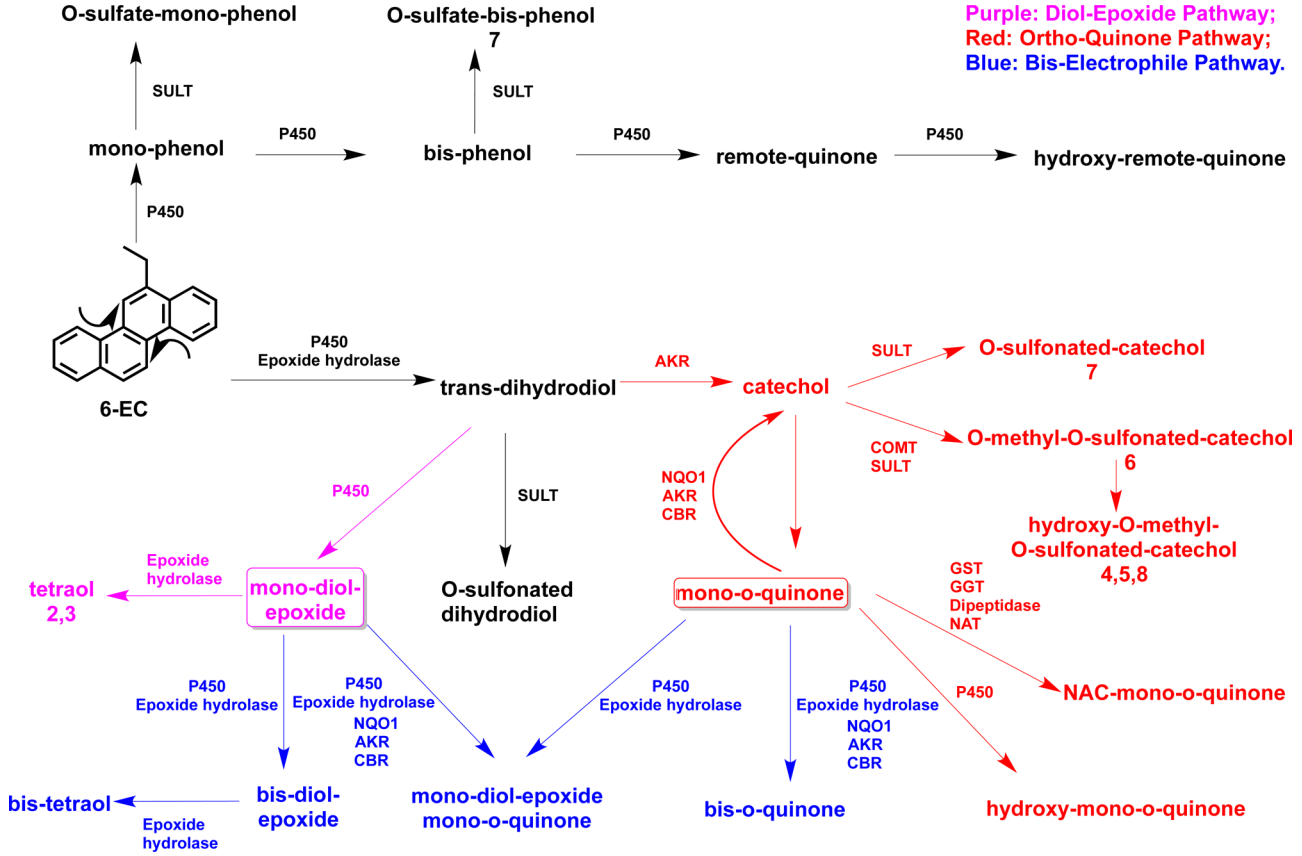

[a]The number of each metabolite corresponds to the metabolites labeled in the UV and fluorescence chromatograms in Figure 1.

DOI: 10.1021/acs.chemrestox.6b00036
Chem. Res. Toxicol. 2016, 29, 991−1002

activation on the two terminal benzo rings to give a bis-diol-epoxide.

O-Monomethyl-catechol-6-EC-ortho-quinone was also detected in HepG2 cells by comparing the extracted ion chromatograms of Orbitrap full scan at 0 and 24 h in the positive ion mode (Figure S6), indicating the occurrence of the formation of a bis-ortho-quinone. In particular, the unique biotransformation involving O-methylation strongly indicated the formation of the catechol, thus confirming the occurrence of the ortho-quinone pathway. Further evidence for the formation of a bis-ortho-quinone came from the detection of 6-EC-bis-ortho-quinone in HepG2 cells when the extracted ion chromatograms of Orbitrap full scan at 0 and 24 h in the positive ion mode were compared (Figure S7).

DISCUSSION

6-EC is a representative regioisomer of C2-chrysenes present in crude oil that may enter the food chain after oil spills. We examined its metabolism in human HepG2 cells knowing that human exposure pathways involve ingestion. Human HepG2 cells were selected as an alternative to human hepatocytes due to the limitations of the latter, for instance, scarce availability, shorter life span, phenotypic instability, and higher individual variability.

We proposed four potential pathways of 6-EC metabolic activation: formation of diol-epoxides, ortho-quinones, bis-electrophiles, and ethanesulfonates. We found evidence for the first three pathways but no evidence for activation on the ethyl side chain involving hydroxylation and subsequent sulfonation. Representative metabolites of 6-EC from the pathways of activation were detected and identified by HPLC-UV-FLR and LC-MS/MS (Table 4). Metabolites 2 and 3 in Figure 1 were identified as isomers of a tetraol. Metabolites 4, 5, and 8 in Figure 1 were identified as isomers of a monohydroxy-O-monomethyl-O-monosulfonated-catechol. Metabolite 6 in Figure 1 was identified as an O-monomethyl-O-monosulfonated-catechol. Metabolite 7 in Figure 1 was identified as an O-monosulfonated-catechol or an O-monosulfonated-bis-phenol. Metabolites 1 and 9 in Figure 1 remain unassigned.

On the basis of the peak areas of the metabolites on UV and FLR chromatograms, the major potential metabolic activation pathways of 6-EC in human HepG2 cells involved formation of diol-epoxides and ortho-quinones (Scheme 2). We also found evidence for the potential metabolic activation of 6-EC on both bay regions to form bis-electrophiles containing a mono-diol-epoxide and a mono-ortho-quinone within the same structure, bis-diol-epoxides, and bis-ortho-quinones (Scheme 2). We suspect that these metabolites were underdetected probably due to the potential of bis-electrophiles to form protein and DNA cross-links.

We did not find any evidence for hydroxylation on the ethyl group side chain at C6 followed by formation of sulfate in human HepG2 cells, which is consistent with the previous findings that hydroxymethylation of 5-methylchrysene and 6-methylchrysene (6-MC) is not an important metabolic activation pathway in humans.[6,11] Monodehydrated O-monosulfonated-6-EC-dihydrodiol shown in Figure 2 has an identical nominal mass as that of the sulfate conjugate of side chain monohydroxy-6-EC. However, the fragmentation pattern in Figure 2 shows the loss of the sulfate group and the subsequent loss of the CH_3 group, which rules out the possibility of side chain hydroxylation on 6-EC.

Metabolic activation of 6-MC via a diol-epoxide pathway has been previously characterized in mouse skin, human liver microsomes, and human lung microsomes.[11−14] In this pathway, 6-MC containing a methyl group located at a non-bay region is activated by P450 1A1 to yield 6-MC-1*R*,2*R*-diol, which is further converted to 6-MC-1*R*,2*S*-diol-3*S*,4*R*-epoxide with relatively weak DNA-binding and carcinogenic properties compared with those of the diol-epoxide generated from 5-methylchrysene containing a methyl group located at a bay region.[14−16] It was also reported that hydroxylation on the methyl group of 6-MC catalyzed by P450 3A4 and 1A2 leads to 6-hydroxy-6-MC without carcinogenic and tumor-initiating activities in mouse skin.[17] However, a large amount of 6-MC was left unmetabolized after incubation in human liver microsomes, and a few metabolites found in significant amounts were unidentified,[11] which may explain why only the diol-epoxide pathway of 6-MC activation was proposed previously. The structure of 6-EC is identical to that of 6-MC except for the length of the side chain; therefore, it was expected that the diol-epoxide pathway of 6-EC would be identified in the present study.

Multiple metabolites were detected which indicated that the ortho-quinone pathway was involved in the potential metabolic activation of 6-EC. Interestingly, O-monomethyl-O-monosulfonated-6-EC-catechols and their monohydroxy products were detected in human HepG2 cells, whereas O-monomethyl-6-EC-catechols were not detected, which could be explained if either the O-monomethyl catechol is rapidly sulfonated or sulfonation proceeds prior to O-methylation. We failed to observe the occurrence of O-monoglucuronidation of 6-EC-catechol, probably due to the low expression level of uridine 5′-diphospho-glucuronosyltransferases in human HepG2 cells.[18]

The enzymes responsible for the potential metabolic activation pathway of 6-EC in human HepG2 cells remain to be identified. Inducible cytochrome P450 1A1 present in human HepG2 cells is probably responsible for the formation of diol-epoxides.[19] Several members of the aldo-keto reductase (AKR) superfamily, including AKR1C1, AK1C2, and AKR1C3, present in human HepG2 cells would oxidize 6-EC trans-dihydrodiols to ortho-quinones.[20−22] However, liver-specific AKR1C4 is absent in human HepG2 cells.[22] AKRs, NAD(P)H:quinone oxidoreductase 1, and carbonyl reductase can all catalyze the redox cycling of ortho-quinones to form intermediate catechols.[23] Formation of 6-EC-diones indicates that subsequent conjugation of the catechols is not completely effective in preventing redox cycling, as predicted earlier in our studies of benzo[*a*]pyrene-7,8-dione.[24] Sulfotransferases (SULTs) and catechol-O-methyltransferase would be responsible for the formation of O-monomethyl-O-monosulfonated-catechols.[25,26] The SULTs that are expressed in human HepG2 cells and likely responsible for O-sulfonation are SULT1A1, 1A2, 1E1, and 2A1.[18] γ-Glutamyltranspeptidase, dipeptidase, and *N*-acetyl transferase would sequentially catalyze the degradation of a GSH-ortho-quinone conjugate to generate the NAC-ortho-quinone conjugate that was detected.[27] Potential dual metabolic activation of 6-EC on both terminal benzo rings was consistent with the previous findings of 5-methylchrysene,[6] which further confirmed that P450 1A1 and AKRs can work separately or together in the metabolic activation of chrysene derivatives containing two bay regions to form bis-electrophiles.

Elucidation of the metabolic pathways of 6-EC in human liver cells can be used to identify exposure biomarkers of 6-EC

DOI: 10.1021/acs.chemrestox.6b00036
Chem. Res. Toxicol. 2016, 29, 991−1002

that could be used for biomonitoring human urine and plasma. Our earlier studies on the metabolic activation of 5-methylchrysene indicated metabolites in common with those found in the present study, i.e., tetraols and catechol conjugates. In particular, O-sulfonated-catechols observed in both studies could be biomarkers due to the intense molecular ions in the negative ion mode and the characteristic loss of the sulfate group (80 amu) in MS^2 spectra. By developing a panel of biomarkers for petrogenic PAH exposure, requisite specificity and sensitivity will likely increase as opposed to measuring a single analyte.[28] These biomarkers have the potential for monitoring the consumption of oil-contaminated seafood in humans.

■ ASSOCIATED CONTENT

Supporting Information

The Supporting Information is available free of charge on the ACS Publications website at DOI: 10.1021/acs.chemrestox.6b00036.

Excitation and emission wavelength spectra of 6-EC (Figure S1); UV spectra of 6-EC and metabolites 1−9 in HepG2 cells (Figure S2); and extracted ion chromatograms of Orbitrap full scan for 6-EC-dihydrodiols and monodehydrated 6-EC-dihydrodiols (Figure S3), monodehydrated 6-EC-tetraol and bis-dehydrated 6-EC-tetraol (Figure S4), bis-tetraol (Figure S5), O-monomethylcatechol-6-EC-ortho-quinone (Figure S6), and 6-EC-bis-ortho-quinone (Figure S7) detected in HepG2 cells (PDF)

■ AUTHOR INFORMATION

Corresponding Author

*E-mail: penning@upenn.edu. Telephone: (215) 898-9445. Fax: (215) 573-0200.

Funding

This publication was made possible by Deepwater Horizon Research Consortia grant numbers U19 ES020676-04 and P30 ES013508 (T.M.P.) from the National Institute of Environmental Health Sciences (NIEHS), NIH, DHHS. Its contents are solely the responsibility of the authors and do not necessarily represent the official views of the NIEHS or NIH.

Notes

The authors declare no competing financial interest.

■ ABBREVIATIONS

AKR, aldo-keto reductase; P450, cytochrome P450; Cys, cysteine; Cys-Gly, cysteinylglycine; ESI, electrospray ionization; GSH, glutathione; HPLC-UV-FLR, high-performance liquid chromatography ultraviolet fluorescence; LC-MS/MS, liquid chromatography tandem mass spectrometry; 6-EC, 6-ethylchrysene; 6-MC, 6-methylchrysene; NAC, *N*-acetyl-L-cysteine; PAH, polycyclic aromatic hydrocarbon; SULTs, sulfotransferases

■ REFERENCES

(1) Joye, S. B., MacDonald, I. R., Leifer, I., and Asper, V. (2011) Magnitude and oxidation potential of hydrocarbon gases released from the BP oil well blowout. *Nat. Geosci. 4*, 160−164.

(2) Atlas, R. M., and Hazen, T. C. (2011) Oil biodegradation and bioremediation: a tale of the two worst spills in US history. *Environ. Sci. Technol. 45*, 6709−6715.

(3) Goldstein, B. D., Osofsky, H. J., and Lichtveld, M. Y. (2011) The gulf oil spill. *N. Engl. J. Med. 364*, 1334−1348.

(4) Ylitalo, G. M., Krahn, M. M., Dickhoff, W. W., Stein, J. E., Walker, C. C., Lassitter, C. L., Garrett, E. S., Desfosse, L. L., Mitchell, K. M., Noble, B. T., Wilson, S., Beck, N. B., Benner, R. A., Koufopoulos, P. N., and Dickey, R. W. (2012) Federal seafood safety response to the Deepwater Horizon oil spill. *Proc. Natl. Acad. Sci. U. S. A. 109*, 20274−20279.

(5) Rothman, N., Poirier, M. C., Baser, M. E., Hansen, J. A., Gentile, C., Bowman, E. D., and Strickland, P. T. (1990) Formation of polycyclic aromatic hydrocarbon-DNA adducts in peripheral white blood cells during consumption of charcoal-broiled beef. *Carcinogenesis 11*, 1241−1243.

(6) Huang, M., Zhang, L., Mesaros, C., Hackfeld, L. C., Hodge, R. P., Blair, I. A., and Penning, T. M. (2015) Metabolism of an alkylated polycyclic aromatic hydrocarbon 5-methylchrysene in human hepatoma (HepG2) cells. *Chem. Res. Toxicol. 28*, 2045−2058.

(7) Huang, M., Zhang, L., Mesaros, C., Zhang, S., Blaha, M. A., Blair, I. A., and Penning, T. M. (2014) Metabolism of a representative oxygenated polycyclic aromatic hydrocarbon (PAH) phenanthrene-9,10-quinone in human hepatoma (HepG2) cells. *Chem. Res. Toxicol. 27*, 852−863.

(8) *Standard Reference Material (SRM) 2779: Gulf of Mexico Crude Oil*, National Institute of Standards and Technology, Gaithersburg, MD, 2012.

(9) John, G. F., Yin, F., Mulabagal, V., Hayworth, J. S., and Clement, T. P. (2014) Development and application of an analytical method using gas chromatography/triple quadrupole mass spectrometry for characterizing alkylated chrysenes in crude oil samples. *Rapid Commun. Mass Spectrom. 28*, 948−956.

(10) Scholz, K., Dekant, W., Volkel, W., and Pahler, A. (2005) Rapid detection and identification of *N*-acetyl-*L*-cysteine thioethers using constant neutral loss and theoretical multiple reaction monitoring combined with enhanced product-ion scans on a linear ion trap mass spectrometer. *J. Am. Soc. Mass Spectrom. 16*, 1976−1984.

(11) Koehl, W., Amin, S., Staretz, M. E., Ueng, Y. F., Yamazaki, H., Tateishi, T., Guengerich, F. P., and Hecht, S. S. (1996) Metabolism of 5-methylchrysene and 6-methylchrysene by human hepatic and pulmonary cytochrome P450 enzymes. *Cancer Res. 56*, 316−324.

(12) Amin, S., Huie, K., Melikian, A. A., Leszczynska, J. M., and Hecht, S. S. (1985) Comparative metabolic activation in mouse skin of the weak carcinogen 6-methylchrysene and the strong carcinogen 5-methylchrysene. *Cancer Res. 45*, 6406−6442.

(13) Amin, S., Huie, K., Balanikas, G., Hecht, S. S., Pataki, J., and Harvey, R. G. (1987) High stereoselectivity in mouse skin metabolic activation of methylchrysenes to tumorigenic dihydrodiols. *Cancer Res. 47*, 3613−3617.

(14) Hecht, S. S., Amin, S., Huie, K., Melikian, A. A., and Harvey, R. G. (1987) Enhancing effect of a bay region methyl group on tumorigenicity in newborn mice and mouse skin of enantiomeric bay region diol epoxides formed stereoselectively from methylchrysenes in mouse epidermis. *Cancer Res. 47*, 5310−5315.

(15) Melikian, A. A., Amin, S., Huie, K., Hecht, S. S., and Harvey, R. G. (1988) Reactivity with DNA bases and mutagenicity toward Salmonella typhimurium of methylchrysene diol epoxide enantiomers. *Cancer Res. 48*, 1781−1787.

(16) Melikian, A. A., Prahalad, K. A., Amin, S., and Hecht, S. S. (1991) Comparative DNA binding of polynuclear aromatic hydrocarbons and their dihydrodiol and bay region diolepoxide metabolites in newborn mouse lung and liver. *Carcinogenesis 12*, 1665−1670.

(17) Amin, S., Juchatz, A., Furuya, K., and Hecht, S. S. (1981) Effects of fluorine substitution on the tumor initiating activity and metabolism of 5-hydroxymethylchrysene, a tumorigenic metabolite of 5-methylchrysene. *Carcinogenesis 2*, 1027−1032.

(18) Westerink, W. M., and Schoonen, W. G. (2007) Phase II enzyme levels in HepG2 cells and cryopreserved primary human hepatocytes and their induction in HepG2 cells. *Toxicol. In Vitro 21*, 1592−1602.

DOI: 10.1021/acs.chemrestox.6b00036
Chem. Res. Toxicol. 2016, 29, 991−1002

(19) Burczynski, M. E., and Penning, T. M. (2000) Genotoxic polycyclic aromatic hydrocarbon ortho-quinones generated by aldo-keto reductases induce CYP1A1 via nuclear translocation of the aryl hydrocarbon receptor. *Cancer Res. 60*, 908−915.
(20) Palackal, N. T., Burczynski, M. E., Harvey, R. G., and Penning, T. M. (2001) The ubiquitous aldehyde reductase (AKR1A1) oxidizes proximate carcinogen trans-dihydrodiols to o-quinones: potential role in polycyclic aromatic hydrocarbon activation. *Biochemistry 40*, 10901−10910.
(21) Palackal, N. T., Lee, S. H., Harvey, R. G., Blair, I. A., and Penning, T. M. (2002) Activation of polycyclic aromatic hydrocarbon trans-dihydrodiol proximate carcinogens by human aldo-keto reductase (AKR1C) enzymes and their functional overexpression in human lung carcinoma (A549) cells. *J. Biol. Chem. 277*, 24799−24808.
(22) Steckelbroeck, S., Oyesanmi, B., Jin, Y., Lee, S. H., Kloosterboer, H. J., and Penning, T. M. (2005) Tibolone metabolism in human liver is catalyzed by 3alpha/3beta-hydroxysteroid dehydrogenase activities of the four isoforms of the aldo-keto reductase (AKR)1C subfamily. *J. Pharmacol. Exp. Ther. 316*, 1300−1309.
(23) Shultz, C. A., Quinn, A. M., Park, J. H., Harvey, R. G., Bolton, J. L., Maser, E., and Penning, T. M. (2011) Specificity of human aldo-keto reductases, NAD(P)H:quinone oxidoreductase, and carbonyl reductases to redox-cycle polycyclic aromatic hydrocarbon diones and 4-hydroxyequilenin-o-quinone. *Chem. Res. Toxicol. 24*, 2153−2166.
(24) Huang, M., Liu, X., Basu, S. S., Zhang, L., Kushman, M. E., Harvey, R. G., Blair, I. A., and Penning, T. M. (2012) Metabolism and distribution of benzo[*a*]pyrene-7,8-dione (B[*a*]P-7,8-dione) in human lung cells by liquid chromatography tandem mass spectrometry: detection of an adenine B[*a*]P-7,8-dione adduct. *Chem. Res. Toxicol. 25*, 993−1003.
(25) Zhang, L., Jin, Y., Chen, M., Huang, M., Harvey, R. G., Blair, I. A., and Penning, T. M. (2011) Detoxication of structurally diverse polycyclic aromatic hydrocarbon (PAH) o-quinones by human recombinant catechol-O-methyltransferase (COMT) via O-methylation of PAH catechols. *J. Biol. Chem. 286*, 25644−25654.
(26) Zhang, L., Huang, M., Blair, I. A., and Penning, T. M. (2012) Detoxication of benzo[*a*]pyrene-7,8-dione by sulfotransferases (SULTs) in human lung cells. *J. Biol. Chem. 287*, 29909−29920.
(27) Blair, I. A. (2010) Analysis of endogenous glutathione-adducts and their metabolites. *Biomed. Chromatogr. 24*, 29−38.
(28) Firpo, M. A., Boucher, K. M., and Mulvihill, S. J. (2014) Prospects for developing an accurate diagnostic biomarker panel for low prevalence cancers. *Theor. Biol. Med. Modell. 11*, 34.

DOI: 10.1021/acs.chemrestox.6b00036
Chem. Res. Toxicol. 2016, 29, 991−1002